Fundamenta Informaticae 175 (2020) 281–299
DOI 10.3233/FI-2020-1957
IOS Press

Network Controllability Analysis of Three Multiple-myeloma Patient Genetic Mutation Datasets

Jose Angel Sanchez Martin
Department of Information Systems
Polytechnic University of Madrid, Spain
joseangel.sanchez.martin@alumnos.upm.es

Ion Petre*
Department of Mathematics and Statistics
University of Turku, Finland and
National Institute for Research and Development
in Biological Sciences, Romania
ion.petre@utu.fi

Abstract. Network controllability focuses on the concept of driving the dynamical system associated to a directed network of interactions from an arbitrary initial state to an arbitrary final state, through a well-chosen set of input functions applied in a minimal number of so-called input nodes. In earlier studies we and other groups demonstrated the potential of applying this concept in medicine. A directed network of interactions may be built around the main known drivers of the disease being studied, and then analysed to identify combinations of drug targets controlling survivability-essential genes in the network. This paper takes the next step and focuses on patient data. We demonstrate that comprehensive protein-protein interaction networks can be built around patient genetic data, and that network controllability can be used to identify possible personalised drug combinations. We discuss the algorithmic methods that can be used to construct and analyse these networks.

Keywords: Network controllability, personalised medicine, multiple myeloma, mutated genes, essential genes, drug target genes.

*Address for correcpondence: Department of Mathematics and Statistics, University of Turku, Finland

1. Introduction

Precision medicine is centred on the general objective to integrate a patient's own data with knowledge about basic genetic and biological mechanisms of disease to identify her own disease activation pathways and based on them, potentially new therapeutic strategies uniquely suited to that patient [1], [2]. Mathematical models can integrate knowledge on patient genetic abnormalities, on tumour drivers, and pharmacokinetics of drug combinations, to build comprehensive disease- and tumour-specific models. Such models can then be analysed as dynamic complex systems based on directed graphs to gain insights into the vulnerabilities of the tumour signalling network [3]. This approach can be personalised in that the study is driven by the patient's own data to identify her own unique molecular network of disease. Such networks are discussed in this paper as directed graphs. The patient's own mutated genes are represented in the network as vertices. The edges represent interactions between the genes (or in fact, without the risk of confusion, between the proteins encoded by the genes). Since we want to describe also multi-step interactions between the patient's mutated genes, additional vertices may be added to the network, representing genes that influence or are being influenced by the mutated genes. We take an elementary approach to representing such interactions as directed graphs and ignore a number of additional attributes of the edges (e.g., type of interaction, strength, mechanistic details) and of the vertices (e.g., copy number, activation status, the details of the mutation).

There is a wide spectrum of modelling methods that may be used to analyse a disease network and the dynamical systems associated to it: ODE-based models [4], [5], Boolean and Bayesian models [6], [7], executable models [8], network models [9, 10, 11], and many others. A major focus is on finding novel personalised combinatorial drug therapies [12]. A very promising method that we [13, 14] and others, e.g., [15, 16, 17], successfully used in this context is network controllability [18], with many interesting applications also outside medicine, e.g., in directing the moves of a C.elegans nematode [19], [20]. In brief, the concept of network controllability is that the dynamical system associated to the network may be driven between arbitrary configurations by fixing the dynamic of a small subset of its vertices (called input or driver nodes) to a suitable set of functions. The appeal for the applications in medicine comes from considering the input vertices from those encoding for genes that are targetable by available drugs. A solution to the network controllability problem in this case gives a combination of such vertices (and hence a combination of available drugs) that may change the dynamics of the network between arbitrary configurations, i.e., a (theoretical) suggestion for a personalised combinatorial drug therapy.

We discuss in this paper the applicability of network controllability to patient data. Previous studies have focused mostly on disease networks (constructed around generic disease drivers and typical mutated genes), see, e.g., [13]. In this paper we show that the method is also applicable to patient- and tumour-data. We build and analyse three networks around the mutation data of three multiple-myeloma tumour samples, each from a different patient, based on the data from [21]. We show that network controllability can offer a variety of personalised drug combination options, including standard multiple-myeloma drugs, as well as suggestions for potentially useful new drug targets.

The paper is structured as follows. In Section 2 we discuss the network controllability problems and some algorithmic heuristics for it. In Section 3 we discuss the data we used to generate the patient disease networks. In Section 4 we discuss the results we obtained for the three cases we investigated.

We conclude in Section 5 with some thoughts on the applicability of our methods for personalised medicine.

2. A brief introduction to network controllability

2.1. Theory

We give here a brief introduction into the theory of network controllability. For more details we refer to [14]. We discuss here the continuous formulation of the controllability problem; a discrete version also exists.

All vectors are considered in the following to be column vectors. This makes all matrix-vector multiplications below well defined.

A linear (time-invariant) dynamical system is an n-dimensional ($n \geq 1$) vector x of real functions $x : \mathbb{R} \to \mathbb{R}^n$ defined through the system of ordinary differential equations

$$\frac{dx(t)}{dt} = Ax(t), \tag{1}$$

where $A \in \mathbb{R}^{n \times n}$. Such a system can be thought of as a continuous-time, n-state transition system, with A the (time-invariant) state transition matrix describing how each of these states are influencing the dynamics of the other states. Specifically, the (i, j)-entry $a_{i,j}$ of matrix A describes the weight of the influence of node j over node i.

When an external input u is introduced in this system in order to (linearly) influence it, Equation (1) develops into

$$\frac{dx(t)}{dt} = Ax(t) + Bu(t), \tag{2}$$

where $u : \mathbb{R} \to \mathbb{R}^m$, $m \geq 1$, is the external m-dimensional input vector, thought of as a time-dependent set of functions influencing some of the states of the dynamical system. This influence is described through matrix $B \in \mathbb{R}^{n \times m}$: the (i, j)-entry $b_{i,j}$ of B describes the weight of the influence of input u_j over the internal state x_i. An internal state x_i such that there is $1 \leq j \leq m$ with $b_{i,j} \neq 0$ is called a *driven* state. The intuition is that such a state is driven through a direct influence by one of the inputs. The other, non-driven states are also indirectly influenced by the inputs through the cascading influence of the internal nodes over each other, as described by matrix A.

In the additional case where the system also exports a set of $k \geq 1$ output functions $y : \mathbb{R} \to \mathbb{R}^k$, the system (2) becomes

$$\frac{dx(t)}{dt} = Ax(t) + Bu(t), \qquad y(t) = Cx(t) \tag{3}$$

where $C \in \mathbb{R}^{k \times n}$ is the output matrix specifying how each of the k outputs depends on the n variables of the system. We refer to systems of form (3) as the linear dynamical system (A, B, C).

Throughout this paper we are interested in the simpler case where the output function is of the form $y(t) = (x_{t_1}(t), x_{t_2}(t), \ldots, x_{t_k}(t))^T$. In other words, the output functions are simply collecting

the values from some *target* nodes $T = \{t_1, t_2, \ldots, t_k\} \subseteq \{1, 2, \ldots, n\}$. This means that matrix $C \in \{0,1\}^{k \times n}$ is defined in the following way: $c_{i,j} = 1$ if and only if $i = j \in T$. We denote C_T the output matrix associated in this way to target set T.

We illustrate in Figure 1 the structure of a network in the controllability setup, including the interactions corresponding to matrices A, B and C, the input nodes u, the internal nodes x, the driven nodes, the target nodes $\mathcal{T}$, and the output nodes y.

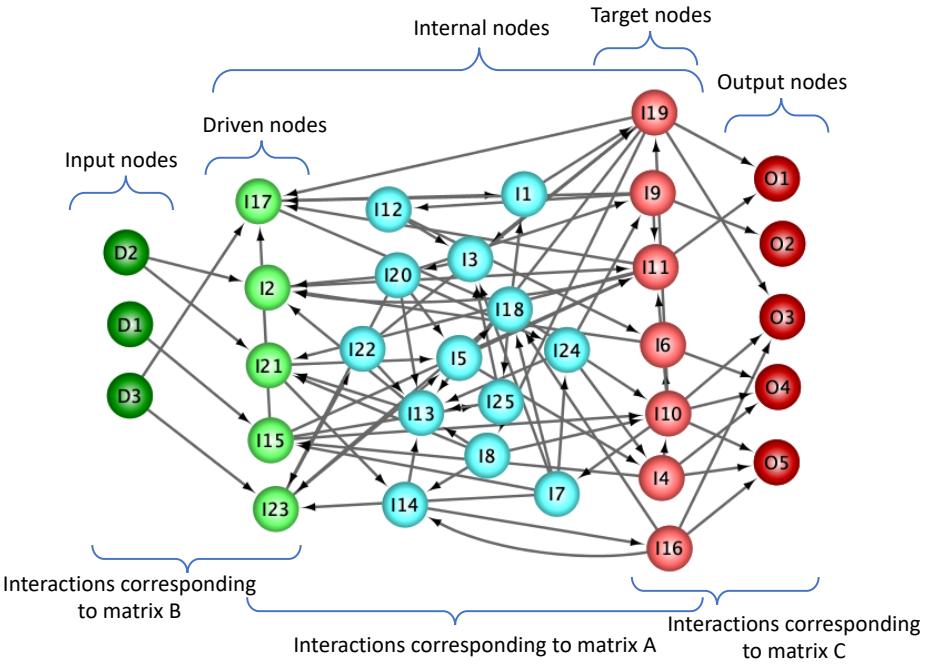

Figure 1. The structure of a network in the controllability setup: the interactions corresponding to matrices A, B and C, the input nodes, the driven nodes, the internal nodes, the target nodes, and the output nodes.

Given a target set T, a linear dynamical system (A, B, C_T) is said to be *target controllable* if for any initial condition $x_0 \in \mathbb{R}^n$ and any $\tilde{y} \in \mathbb{R}^k$, there is an input vector $u_{x_0,\tilde{y}} : \mathbb{R} \to \mathbb{R}^m$, $m \geq 1$ such that $y(\tau) = \tilde{y}$, for some $\tau \geq 0$. Intuitively, a linear dynamical system being target controllable means that for any initial configuration x_0 of the system and for any configuration $\tilde{y}$ of the target states, there is a suitable set of input functions able to "drive" the target states to $\tilde{y}$ in finite time. The input functions may differ depending on x_0 and $\tilde{y}$.

We discuss the following two questions:

Q_1. Decide if a given linear dynamical system (A, B, C_T) is controllable.

Q_2. For $A \in \mathbb{R}^{n \times n}$ and $C_T \in \mathbb{R}^{k \times n}$, find the smallest $m \geq 1$ and $B \in \mathbb{R}^{n \times m}$ such that (A, B, C_T) is target controllable.

Question Q_1 has an elegant answer in the form of the following algebraic result.

Theorem 2.1. (Kalman's condition [22]) A linear dynamical system (A, B, C_T) is controllable if and only if $rank[C_TB, C_TAB, C_TA^2B, \ldots, C_TA^{n-1}B] = |T|$.

Kalman's condition is an elegant complete solution to the controllability problem. Its applicability in practice is however limited because of two reasons. First, the matrices A and B have to be completely satisfied, so that the rank of the *controllability matrix* $[C_TB, C_TAB, C_TA^2B, ..., C_TA^{n-1}B]$ of (A, B, C_T) can be calculated. This means in particular that the weight of all internal interactions of the system must be known. This is a major limitations for *observed* systems, whose interactions are often partially unknown and not directly measurable. Second, even if all the internal interactions were known and measured, Kalman's condition is highly sensitive on the values of the entries of matrices A and B. This is a major limitations for observed systems, whose internal settings can only be measured or estimated with finite precision, leading to conflicting results on Kalman's condition for numerical settings within the range of the measurement/estimation errors. This motivates the question of whether the controllability of a system could be defined in terms of its structure, rather than its numerical setup. We discuss this in the following in terms of the *structural controllability* problem.

We say that two matrices $X, Y \in \mathbb{R}^{u\times v}$, $u, v \geq 1$ are *structurally equivalent* if for all $1 \leq i \leq u$, $1 \leq j \leq v$, $X_{i,j} \neq 0$ if and only if $Y_{i,j} \neq 0$. Equivalently, if we consider the two (weighted) graphs having X and Y as their adjacency matrices, X, Y are structurally equivalent if and only if their two (weighted) graphs have exactly the same set of edges (with potentially different weights).

We say that a linear dynamical system (A, B, C_T) is *structurally controllable* if and only if there are matrices A', B' structurally equivalent to A and B, resp., such that (A', B', C_T) is controllable. In other words, a linear dynamical system is structurally controllable if and only if by replacing arbitrarily any of its non-zero coefficients with other non-zero coefficients, the system can be made controllable. The intuition is that by doing so, the structure of the associated graph remains unchanged.

The following surprising result shows that controllability is in fact a structural concept, and not a numerical one. We recall based on [23] that in mathematical analysis a *thin* set is a subset of $\mathbb{R}^n$ with the property that each element of the set has a neighbourhood on which some non-zero holomorphic function vanishes. In particular, a thin set is nowhere dense.

Theorem 2.2. ([24]) If a linear dynamical system (A, B, C_T) is structurally controllable, then $(A'$, $B', C_T)$ is controllable for all matrices A' and B' equivalent to A and B, resp., except a thin subset of $\mathbb{R}^{n\times n} \times \mathbb{R}^{n\times m}$.

Intuitively, Theorem 2.2 shows that question Q1 on the controllability of a linear dynamical system is in fact a question about its structure, i.e., about the directed graph (or network) associated to it, defined in the following way. Let $\mathcal{B} = \{1', 2', \ldots, m'\}$ be the set of *input* nodes, $\mathcal{A} = \{1, 2, \ldots, n\}$ be the set of *internal* nodes, and $\mathcal{T} \subseteq \mathcal{A}$ the set of target nodes. The network associated to the linear dynamical system $(A, B, C_\mathcal{T})$ has as its set of vertices $\mathcal{A}\cup\mathcal{B}$, with $\mathcal{T}$ a subset of it. Its set of (directed) edges consists of two types: the input edges $\{(j', i) \mid j' \in \mathcal{B}, i \in \mathcal{A}, b_{i,j} \neq 0\}$ and the internal edges $\{(j, i) \mid i, j \in \mathcal{A}, a_{i,j} \neq 0\}$. We also define the set of *driven* nodes $\{i \in \mathcal{A} \mid \exists j' \in \mathcal{B} : b_{i,j} \neq 0\}$, i.e., the set of nodes of $\mathcal{A}$ adjacent to the input node set $\mathcal{B}$.

The following result describes structural controllability in terms of a simple property of the associated network.

Theorem 2.3. ([25]) If the linear dynamical system (A, B, C_T) with $A \in \mathbb{R}^{n\times n}$, $B \in \mathbb{R}^{n\times m}$, $C_T \in \mathbb{R}^{k\times n}$ is structurally controllable, then in its associated network there is a set of k paths starting in the input nodes and ending in the target nodes, in such a way that no two paths intersect at the same distance from their end points.

Theorem 2.3 gives the foundation of the algorithmic solution to question Q2, discussed in the following section.

2.2. Algorithmics

We discuss now question Q2, of finding a minimum number of input nodes making the linear dynamical system controllable. We follow here the presentation of [14]. Also, thinking of the application to selecting drug combinations, we formulate a version of the controllability problem where the set of driven nodes should be selected as much as possible from a given set of *preferred driven nodes*. A similar discussion is also in [17]. In our applications the preferred driven nodes will be considered to be genes that can be targeted by currently available drugs, hence our stress on including as many of such genes as possible in the set of driven nodes offered by our solution to Q_2. We reformulate question Q_2 as follows:

Q_2' **(Constrained structural target controllability).** Let $A \in \mathbb{R}^{n\times n}$, $C_T \in \mathbb{R}^{k\times n}$. Let also $D \subseteq \{1, 2, \ldots, n\}$ be the set of preferred driven nodes. Find the smallest $m \geq 1$ and $B \in \mathbb{R}^{n\times m}$ such that:

1. (A, B, C_T) is target controllable and
2. $|\{i \in D \mid \exists j \in \{1, 2, \ldots, m\} : b_{i,j} \neq 0\}|$ is maximal.

It has been proved in [14] that the Q_2' problem is NP-complete. A heuristic algorithm to give an approximate solution is also given in [14], formulated in terms of the associated network problem, based on Theorem 2.3. The objective of the algorithm is to find a set of k paths ending in T and starting from a minimal number of driven nodes, selected as much as possible from the set of preferred driven nodes. A minimum set of (new) input nodes is introduced as initial nodes for these paths, in such a way that Theorem 2.3 holds. This also defines matrix B. The solution is based on an iterated maximal matching algorithm as follows.

Algorithm to find an approximation of a solution to Q_2' [14]. We are given a network G with vertices A, a set of targets $T \subseteq A$ of cardinality k and a set of preferred driven nodes $D \subseteq A$. We seek a set of k paths ending in T and starting from a minimal number of nodes, selected as much as possible from the set of preferred driven nodes. One more step then gives the final set of driver nodes and matrix B, as explained above. In the description below we omit this final step because the focus is on finding drug target nodes, with the set of drugs acting on them left to be documented from the DrugBank database [26]. Skipping the additional step of mathematical optimisation helps to avoid predictions of hypotehtical "super-drugs", able to act simultaneously on many diverse targets.

We say that a set of nodes X *dominates* another set of nodes Y in a directed graph, if all nodes in Y are successors of some nodes in X.

Step 1. Let $T' = T$ be the current set of targets to be matched, $I = \emptyset$ the current set of initial nodes for the control pathways.

Step 2. For up to n steps or until T' becomes the empty set, repeat the following. Select a set of predecessors T'' of T' in G dominating a maximal subset of T', such that no two nodes in T' share a selected predecessor. Add to I the nodes of T' not dominated by T'' and let $T' = T''$.

Output Add all remaining nodes in T' to I and output I as the set of driven nodes.

Note that Step 2 of the algorithm allows for the choice of any set of predecessors T'' satisfying the conditions formulated in the algorithm. This allows a randomised implementation of the algorithm, as done in [27]. It also allows for several heuristics to support the objective of selecting as many input nodes from T as possible. The obvious one is to select in T'' in each step a maximal number of nodes from D. Several other heuristics are formulated in [14] and are implemented in [27].

3. Data

We discuss in this section the data we used to generate the three networks we analysed.

3.1. Patient mutation data

The genetic mutation data used in our study is from [21]. The provided dataset includes 203 different tumour samples with thorough information about the mutated genes, the specific details of the mutation and the patients' characteristics, such as age, race and gender among others. We included in our study only the information about the mutated genes in each sample. Table 4 summarises the mutation data of [21].

Table 1. Patient mutation dataset statistics.

Number of tumour samples	203
Number of genes mutated in at least one of the samples	14 562
Number of genes mutated in at least 10 % of the samples	403
Number of genes mutated in at least 20 % of the samples	1

We chose for our analysis tumour samples 389, 343, and 191. We chose sample 389 because it contains the largest number of mutated genes. We chose samples 343 and 191 for the diversity of the network controllability analysis results, helping us to demonstrate the feasibility of the approach in the medical context. For tumour 343 our results, discussed below, include both standard multiple myeloma drugs, as well as a gene not targeted by current drugs, that is predicted to have strong effect on this tumour: it controls 12 essential genes in the network. For tumour 191 we identified a multiple myeloma drug that is not typically used in first-line treatments for this disease, yet it controls 11 essential genes in this network.

3.2. Multiple myeloma survivability-essential genes

A gene is called *survivability-essential* for a cell if knocking it out leads to cell death [28, 29]. Through the *CRISPR-Cas9*-based genome editing analysis, a wide range of results became recently available for *disease-specific survivability-essential gene*, see [30, 31, 32]: these are genes whose knocking out leads to cell death in diseased cells, but appears neutral in healthy cells. The concept of disease-specific essential genes is immediately amenable to investigations for potential drug targeting. Unfortunately, most such genes are untargettable by currently available drugs. Our conceptual alternative to this problem is to use network controllability to find combinations of targets of available drugs, that can control the disease-specific essential genes included in the tumour-specific network being analysed, if any exist. This is the objective of our analysis, described in Section 4. The list of 70 multiple myeloma-specific essential genes we used is from [32, 33, 34] and is shown in Table 2.

Table 2. Multiple myeloma: disease-specific surviavability-essential genes [32, 33, 34].

AGTRAP	CUL9	IKZF3	NDC80	PSMA4	RPL38	TRIM68
AURKB	EFNA2	IRF4	NFKB1	PSMA6	RRM1	TUBGCP6
CARS	EIF3C	KIF11	NFKB2	PSMC3	RSF1	UBB
CCND2	EIF4A3	KIF18A	NUF2	PSMC4	SF3A1	UBQLNL
CDK11	GNRH2	KIFC2	PCDH18	PSMC5	SLC25A23	ULK3
CDK11A	GPR77	LEPROT	PIM2	RAB11A	SNRPA1	USP36
CDK11B	HIP1	MAF	PLK1	RELA	SNW1	USP8
CKAP5	IK	MCL1	PRPF8	RELB	TNK2	WBSCR22
COPB2	IKBKB	MED14	PSMA1	RGAG1	TPMT	WEE1
CSNK1A1	IKZF1	MED15	PSMA3	RPL27	TRIM21	XPO1

3.3. Multiple myeloma drug targets

The input node subset in the network controllability heuristics is constrained to the targets of the drugs used in the standard therapy lines for multiple myeloma. With this selection, the algorithm gives preference to the control pathways starting from such nodes, if any are found in the network being analysed. This will maximise the number of drugs offered by our analysis as (theoretical) suggestions for treatment of the tumours modelled by our networks. The list of the targets of the standard multiple-myeloma drugs is in Table 3, with the data coming from [26, 35]. In the case of drugs having several targets, we list all of them.

Table 3. The targets of the drugs used in standard therapy lines for multiple myeloma [26, 35].

ANXA1	CRBN	HSD11B1	NOS2	NR3C1	PSMB2	PSMB9	TNF	TUBA4A
CD38	FGFR2	NFKB1	NR0B1	PSMB1	PSMB5	PTGS2	TNFSF11	TUBB
CDH5	GSR	NOLC1	NR1I2	PSMB10	PSMB8	SLAMF7	TOP2A	

3.4. Protein-protein interaction data

The edges of the network were constructed based on data on protein-protein interactions coming from several public pathway databases: *KEGG* [36], *OmniPath* [37], *InnateDB* [38] and *Signor* [39]. We only used interactions that can be interpreted as *directed* influences, such as protein activation and inhibition. Each of these datasets comes in its own format, making it quite challenging to integrate their data into a single network. We generated networks separately using each of them, and then integrated them into a single network as described in Section 3.5.

3.5. Patient-specific protein-protein interaction networks

The networks associated to each of the patients (tumour samples) were constructed using the application *NetControl4BioMed* [27], freely available at [40]. This is a bioinformatics software tool which generates large protein-protein interaction networks around a given set of genes. In our case, the initial set of genes was the mutated genes in each of the three samples we analysed. The application can generate such networks based on interaction data from *KEGG*, *OmniPath*, *InnateDB* and *Signor*. We included in our networks all the edges between these genes. We also included all paths of length up to three (a parametric value of *NetControl4BioMed*) between these genes, and added all the intermediary new vertices to the network. For each sample we generated separate networks based on each of these four interaction databases. We combined them offline through graph union, with the matching done on vertices, based on their gene name annotation. We then eliminated all isolated nodes from the networks. The three networks are quite different in size, consequence of the different numbers of the mutated genes in each sample, and their connectivity in the interaction databases we used. A summary of the networks topology is in Table 4 and in Figures 2-3. The three networks are available at [41] in the *Cytoscape* [42] format.

Table 4. Summary of the topology of the three networks in our study.

	MM-389	MM-343	MM-191
Number of mutated genes	4065	2774	217
Number of nodes	3740	3678	1306
Number of essential gene nodes	25	33	22
Number of multiple myeloma drug target nodes	33	35	36
Number of edges	9471	11520	2576
Network diameter	14	12	10
Characteristic path length	4.7	4.4	4.5
Average number of neighbours	4.6	5.7	3.2

4. Results

We ran the network controllability analysis of *NetControl4BioMed* with the control target set to the list of multiple-myeloma essential genes in Table 2. We used as the preferred set of input nodes the list of multiple myeloma drug targets in Table 3.

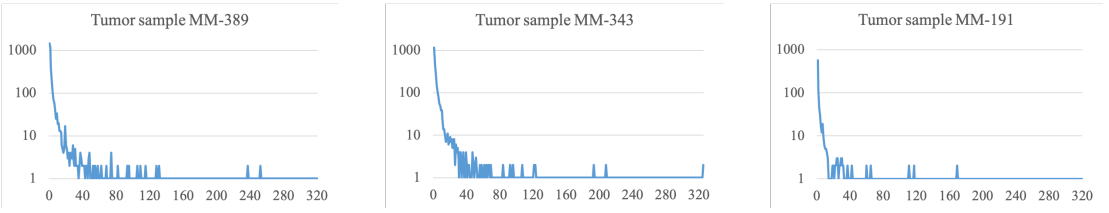

(a) (b) (c)

Figure 2. Out-degree distribution (logarithmic scale) for the network associated to: (a) tumour sample 389; (b) tumour sample 343; (c) tumour sample 191.

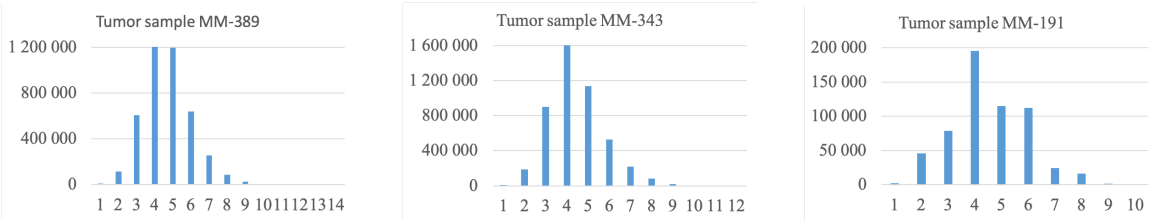

(a) (b) (c)

Figure 3. Shortest path length distribution (a) tumor sample 389; (b) tumor sample 343; (c) tumor sample 191. Note the different scale of the figures.

The result of the network controllability analysis is a set of input nodes that controls the set of control target nodes. For those input nodes that were from the list of preferred inputs in Table 3, we listed the drugs targeting these nodes, as obtained from [26]. As validation we compared this list of drugs predicted by our analysis with the current state of the art regarding the multiple myeloma therapy. We verified if among our predicted drugs there are instances of drugs commonly used in primary and secondary treatments for multiple myeloma. We discuss separately each of the three tumour samples analysed in our study. The network visualisation is done with *Cytoscape* [42], an open source software platform for analysing complex networks and integrating these networks with annotations, gene expression profiles and other data.

4.1. Tumour Sample 389

Tumour sample 389 has 4065 mutated genes, the largest number of mutated genes in the dataset of [21]. The network we built for this sample is shown in Figure 4(a). There are 25 essential genes in this network and the network control analysis found for them the control pathways shown visually in Figure 4(b), listed also in Table 5.

Among the input nodes of these control pathways there were four (*TNF*, *PSMB1*, *HDAC6*, *NFKB1*) that can be targeted by 5 FDA approved multiple myeloma drugs, namely *Thalidomide*, *Pomalidomide*, *Bortezomib*, *Carfilzomib* and *Panobinostat*. This demonstrates that our analysis may help identify several multiple-myeloma drugs targeting the specific interaction network of this tumour sample.

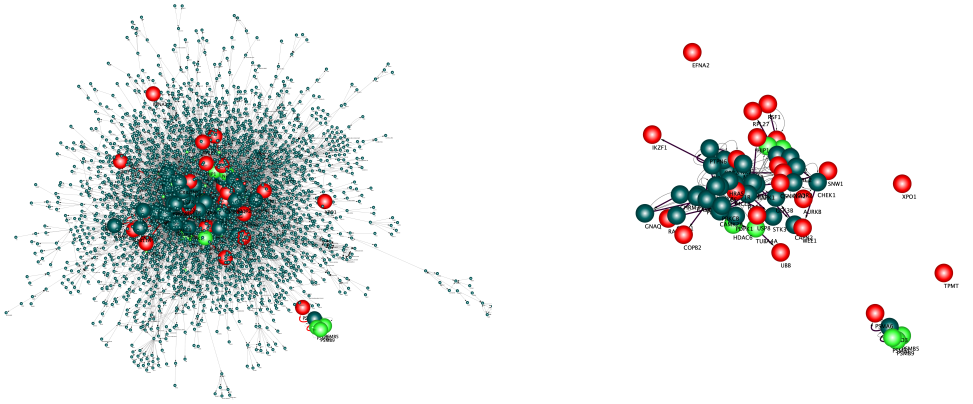

(a) (b)

Figure 4. (a) The protein-protein interaction network associated to tumour sample 389 of [21]; (b) the subnetwork induced by the nodes on the control pathways identified by our analysis. The larger nodes are those on the control pathways. The ones in red are the multiple-myeloma-specific essential genes and the ones in light green are the drug target genes. The edges of the control pathways are thicker.

Table 5. Tumour sample 389: the control pathways to the multiple myeloma essential genes in the network. The essential genes are indicated in bold and the targets of standard multiple myeloma drugs in italics

MIR10A → MAPK1 → CAPN2 → GSK3B → **CSNK1A1** → CHRM3 → GNAQ → PLCE1 → HRAS → RAF1 → STK3 → PRKCA → IRS1 → IGF1R → PDPK1 → PRKCB → CASR → GNAI1 → PLCB1 → PRKCE → **COPB2**
MIR10A → MAPK1 → CAPN2 → GSK3B → **CSNK1A1** → CHRM3 → GNAQ → PLCE1 → HRAS → RAF1 → STK3 → PRKCA → IRS1 → IGF1R → PDPK1 → PRKCB → **RAB11A**
MIR10A → MAPK1 → CAPN2 → GSK3B → **CSNK1A1** → CHRM3 → GNAQ → PLCE1 → HRAS → RAF1 → STK3 → PRKCA → EGFR → HTT → **HIP1**
MIR10A → MAPK1 → CAPN2 → GSK3B → **CSNK1A1** → CHRM3 → GNAQ → PLCE1 → HRAS → RAF1 → CAMK2A → NCOR2 → **SNW1**
MIR10A → MAPK1 → CAPN2 → GSK3B → **CSNK1A1** → CHRM3 → GNAQ → PLCE1 → HRAS → RAF1 → STK3 → PRKCA → EGFR → **TNK2**
MIR10A → GRB2 → SYK → PTPN6 → SRC → **IKBKB** → **PLK1**
MIR10A → GRB2 → SYK → PTPN6 → SRC → **IKBKB**
MIR10A → MAPK1 → CAPN2 → GSK3B → **CSNK1A1**
MIR10A → MAPK1 → **MCL1**
MIR10A → GRB2 → SYK → **IKZF1**
TNF → BIRC2 → *CD40* → TRAF2 → MAP3K14 → **RPL27**
TNF → BIRC2 → CHEK1 → **WEE1**
PSMB1 → *PSMB5* → *PSMB9* → PSMD3 → **PSMA6**
HDAC6 → *TUBA4A* → **UBB**
NFKB1 → **RSF1**
TPMT
AURKB
EFNA2
USP8
XPO1

The control pathway results also suggest that the gene *MIR10A*, which controls 10 essential genes, could be helpful for the treatment of this specific tumour. *MIR10A* is an RNA gene involved in gene regulation, with an affinity for *Hox* genes, important in development processes. There are no approved drugs currently available targeting this gene. We found that *MIR10A* is documented in dozens of recent articles to be differentially expressed in cancer, see, e.g., [43, 44]. This is specifically linked to multiple myeloma, see [45, 46]. We also found that *MIR10A* is succeeded on all the control pathways found by our analysis by either *MAPK1* or by *GRB2*. Both these genes are documented to be linked to multiple myeloma, see [47, 48, 49, 50]. There is even a current clinical trial for multiple myeloma in which *MPAK1* alterations is an inclusion criterion. Since our algorithm searches for a minimization of the number of input nodes, the selection of *MIR10A* to give simultaneous control over both *MPAK1*and *GRB2* is justified.

4.2. Tumor Sample 343

Tumour sample 343 has 2774 mutated genes. Its interaction network has 3678 nodes, out of which 33 were essential genes and 35 were targetable by multiple-myeloma drugs. Our analysis identified three such drugs (*Dexamethasone*, *Prednisone*, *Panobinostat*) to help controlling some of the essential genes. The network is shown in Figure 5(a) and the control pathways shown visually in Figure 5(b), listed also in Table 6.

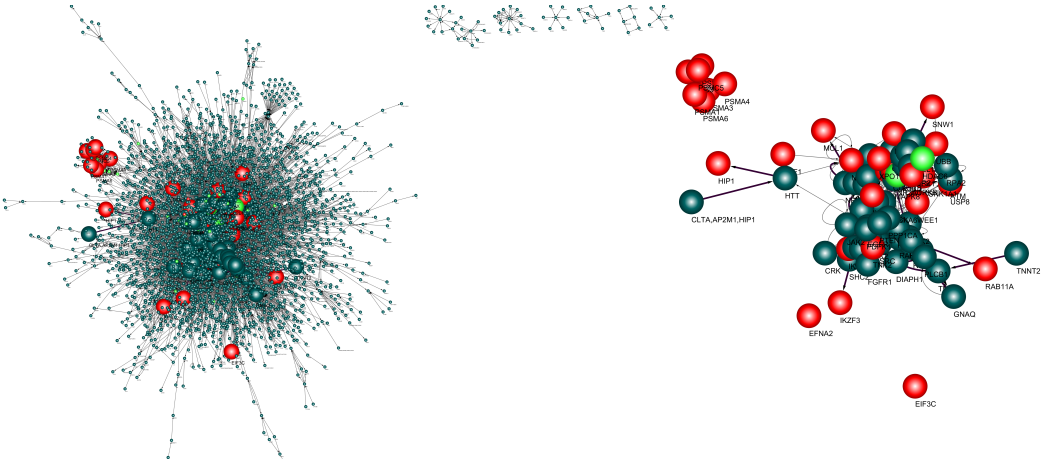

(a) (b)

Figure 5. (a) The protein-protein interaction network associated to tumour sample 343 of [21]; (b) the subnetwork induced by the nodes on the control pathways identified by our analysis. The larger nodes are those on the control pathways. The ones in red are the multiple-myeloma-specific essential genes and the ones in light green are the drug target genes. The edges of the control pathways are thicker.

We also identified that targeting gene *TNNT2* (for which no drug is available) could be highly efficient for this sample, as it leads to controlling 12 essential genes, the highest such number we obtained in our analyses. *TNNT2* encodes for the cardiac muscle troponin T protein, with a role in

Table 6. Tumour sample 343: the control pathways to the multiple myeloma essential genes in the network. The essential genes are indicated in bold and the targets of standard multiple myeloma drugs in italics

TNNT2 → TNC → EGFR → FGFR1 → SHC2 → SRC → PDPK1 → PRKCA → CCR5 → JAK2 → RAF1 → MAP2K1 → MAPK14 → TAB1 → **CSNK1A1** → ATM → RPA2 → CDK7 → **CDK11B**
TNNT2 → TNC → EGFR → FGFR1 → SHC2 → SRC → PDPK1 → PRKCA → CCR5 → JAK2 → RAF1 → MAP2K1 → MAPK14 → TAB1 → **CSNK1A1** → **PLK1**
TNNT2 → TNC → EGFR → FGFR1 → SHC2 → SRC → PDPK1 → PRKCA → CCR5 → JAK2 → RAF1 → MAP2K1 → MAPK14 → TAB1 → **IKBKB**
TNNT2 → TNC → EGFR → FGFR1 → SHC2 → SRC → PDPK1 → PRKCA → GSK3B → TP53 → BAX → BCL2L1 → MAPK8 → **XPO1**
TNNT2 → TNC → EGFR → FGFR1 → SHC2 → SRC → PDPK1 → PRKCA → GRK2 → GNAQ → RHOA → DIAPH1 → **UBB**
TNNT2 → TNC → EGFR → FGFR1 → SHC2 → SRC → PDPK1 → PRKCA → GSK3B → TP53 → CHEK1 → **AURKB**
TNNT2 → TNC → EGFR → FGFR1 → SHC2 → SRC → PDPK1 → PRKCA → MAP2K7 → MAPK10 → **MCL1**
TNNT2 → TNC → EGFR → FGFR1 → SHC2 → SRC → PDPK1 → PRKCA → GSK3B → **CSNK1A1**
TNNT2 → TNC → EGFR → CRK → PTK2 → PTEN → RAC1 → PAK1 → **WEE1**
TNNT2 → TNC → EGFR → MAPK14 → RPS6KA6 → PPP1CA → **IKZF1**
TNNT2 → TNC → EGFR → FGFR1 → GRB2 → **IKZF3**
TNNT2 → TNC → EGFR → **TNK2**
NR3C1 → NFKBIA → ***NFKB1*** → NCOR2 → **SNW1**
AP2M1 → CLTA → HTT → **HIP1**
PLCB1 → PRKCB → **RAB11A**
HDAC6 → **RELB**
EIF3C
EFNA2
PSMA1
PSMA3
PSMA4
PSMA6
PSMC3
PSMC4
PSMC5
RSF1
USP8

regulating muscle contraction in response to alterations in intracellular calcium ion concentrations. Amplifications in this gene is documented in some patients with prostate or breast cancer, see [51], but it is not specifically linked to multiple myeloma. However, *TNNT2*is succeeded on our control pathways by either *TNC* or *EGFR*, both very well documented in the context of multiple myeloma, see [52, 53].

4.3. Tumour Sample 191

Tumour sample 191 has only 217 mutated genes. The network we built for it has 1306 nodes, out of which 22 are essential genes and 36 are targetable by multiple myeloma drugs. The network is shown in Figure 6(a) and the control pathways shown visually in Figure 6(b), listed also in Table 7. Our analysis identified only one multiple myeloma drug (*Dexamethasone*) controlling some of its essential

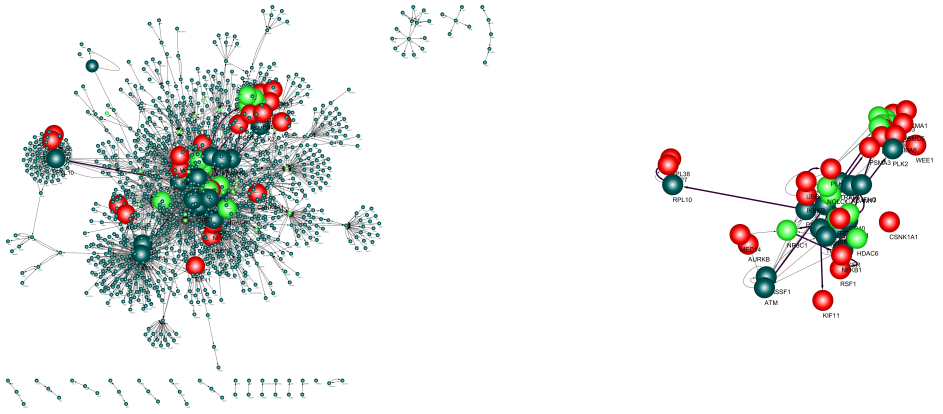

(a) (b)

Figure 6. (a) The protein-protein interaction network associated to tumour sample 191 of [21]; (b) the subnetwork induced by the nodes on the control pathways identified by our analysis. The larger nodes are those on the control pathways. The ones in red are the multiple-myeloma-specific essential genes and the ones in light green are the drug target genes. The edges of the control pathways are thicker.

Table 7. Tumour sample 191: the control pathways to the multiple myeloma essential genes in the network. The essential genes are indicated in bold and the targets of standard multiple myeloma drugs in italics

ANXA1 → RIPK1 → **IKBKB** → PRKCA → ADAM17 → MAPK1 → *HDAC6* → EGFR → *HDAC6* → EGFR → *HDAC6* → EGFR → *PTGS2* → TP53 → PLK2 → **WEE1**
ANXA1 → RIPK1 → **IKBKB** → PRKCA → ADAM17 → MAPK1 → *NR3C1* → ***NFKB1*** → BIRC2 → *CD40* → TRAF6 → *PSMB5* → *PSMB1* → *PSMB2* → **PSMA4**
ANXA1 → RIPK1 → **IKBKB** → PRKCA → ADAM17 → MAPK1 → *NR3C1* → ***NFKB1*** → BIRC2 → *CD40* → TRAF6 → *PSMB5* → *PSMB1* → **PSMC4**
ANXA1 → RIPK1 → **IKBKB** → PRKCA → ADAM17 → MAPK1 → *NR3C1* → ***NFKB1*** → IFNG → *PSMB8* → *PSMB9* → **PSMC3**
ANXA1 → RIPK1 → **IKBKB** → PRKCA → ADAM17 → MAPK1 → *NR3C1* → ***NFKB1*** → BIRC2 → *CD40* → TRAF6 → *PSMB5* → **PSMC5**
ANXA1 → RIPK1 → **IKBKB** → PRKCA → ADAM17 → MAPK1 → *NR3C1* → ***NFKB1*** → **RSF1**
ANXA1 → RIPK1 → **IKBKB** → PRKCA → ADAM17 → MAPK1 → *HDAC6* → **RELB**
ANXA1 → RIPK1 → **IKBKB** → PRKCA → RPL10 → **RPL38**
ANXA1 → RIPK1 → **IKBKB** → IKBKE → **KIF11**
ANXA1 → RIPK1 → **IKBKB** → **PLK1**
ANXA1 → RIPK1 → **IKBKB**
RASSF1 → ATM → **PSMA3**
NOLC1 → **UBB**
AURKB
CSNK1A1
MED14
PSMA1
PSMA6
RPL27

genes. However, this drug is predicted to have an unusual strong effect on this sample, as it controls 11 essential genes, the highest such number in our analyses. *Dexamethasone* is not typically used in the first-line treatment for multiple myeloma, and our analysis offers the prediction that perhaps in this case it could be used as such.

5. Discussion

We discussed in this paper how network controllability can be used to analyse tumour-level data. The set of mutated genes in a tumour sample can be integrated into a directed protein-protein interaction network by considering all interactions between the mutated genes. Such interactions may involve also additional genes. The genes are represented as nodes in the network, and the interactions between them are represented by paths. In this interaction network one can then identify disease-specific survivability-essential genes. Our objective was to find control pathways for them, starting as much as possible from genes targetable by currently available drugs. We demonstrated how the results can be interpreted as suggestions for combinatorial drug therapies.

Generating large interaction networks around the set of mutations of a sample is straightforward through mining current interaction databases. We used the software in [27]. The networks we constructed consisted of between 1000 and 4000 nodes, and 2500 to 12 000 edges. Even larger, more comprehensive networks can be constructed by including longer paths between the mutated genes. The three networks we constructed share similar topological properties, summarised in Table 4 and in Figures 2-3: a power-law distribution of their outdegrees, relatively small diameter, and the shortest path lengths distributed roughly Poisson. These observations are consistent with the networks being scale-free, in line also with observations of [54], [15], and others.

Network controllability turns out to be a powerful tool allowing us to connect disease-specific essential genes with drugs, along with the accompanying pathway of the drug's mechanism of action. With the networks being constructed around the individual mutations of a tumour, this demonstrates the (theoretical) potential of network controllability for personalised drug combination therapies on the tumour level. We showed that some of the results we obtained can be traced back to drugs commonly used in the treatment of multiple myeloma, which can be considered as (indirect, partial) validation of the applicability of controllability for personalised medicine. Furthermore, some other findings seem to suggest novel, highly efficient potential therapeutics: genes that if properly targeted may lead to the control of several essential genes, or drugs typically used on later treatment lines that should perhaps be used upfront. Such findings may be useful to design studies of novel targets and for deciding optimal personalised treatment strategies.

A node in a network may be seen as influential (sometimes called *hub*) if its outdegree is high. They are often singled out by simple topological network analyses and checked for their potential as therapy targets. Our controllability results identify some nodes with high outdegree, but also, somewhat unexpectedly, find drug targets that have a low outdegree but do control a high number of essential genes. This is the case of node/gene *ANXA1* in MM-191 that has outdegree 7, but controls (through longer pathways) 11 essential genes.

Controllability is a topic explored for many types of networks, including Petri nets, see [55]. Their potential in the context of biological or biomedical applications such as those in [56], remains to be explored, along similar lines as those explored in this paper.

Acknowledgments

This work was partially funded by the Romanian National Authority for Scientific Research and Innovation, through the POC grant P_37_257, and by the Polytechnic University of Madrid.

References

[1] Winslow RL, Trayanova N, Geman D, Miller MI. Computational medicine: translating models to clinical care. *Sci Transl Med*, 2012. **4**(158):158rv11. doi:10.1126/scitranslmed.3003528.

[2] 2019. URL `https://www.icpermed.eu/en/activities-vision-paper.php`.

[3] Xie L, Draizen EJ, Bourne PE. Harnessing Big Data for Systems Pharmacology. *Annu Rev Pharmacol Toxicol*, 2017. **57**:245–262. doi:10.1146/annurev-pharmtox-010716-104659.

[4] MacLean AL, Harrington HA, Stumpf MPH, Byrne HM. Mathematical and Statistical Techniques for Systems Medicine: The Wnt Signaling Pathway as a Case Study. *Methods Mol Biol*, 2016. **1386**:405–439. doi:10.1007/978-1-4939-3283-2{_}18.

[5] Gratie DE, Iancu B, Petre I. ODE Analysis of Biological Systems, pp. 29–62. Springer Berlin Heidelberg, Berlin, Heidelberg. ISBN 978-3-642-38874-3, 2013. doi:10.1007/978-3-642-38874-3_2. URL `https://doi.org/10.1007/978-3-642-38874-3_2`.

[6] Wang RS, Saadatpour A, Albert R. Boolean modeling in systems biology: an overview of methodology and applications. *Phys Biol*, 2012. **9**(5):055001. doi:10.1088/1478-3975/9/5/055001.

[7] Bae H, Monti S, Montano M, Steinberg MH, Perls TT, Sebastiani P. Learning Bayesian Networks from Correlated Data. *Scientific Reports*, 2016. **6**(1):25156. doi:10.1038/srep25156. URL `https://doi.org/10.1038/srep25156`.

[8] Bartocci E, Lió P. Computational Modeling, Formal Analysis, and Tools for Systems Biology. *PLOS Computational Biology*, 2016. **12**(1):1–22. doi:10.1371/journal.pcbi.1004591. URL `https://doi.org/10.1371/journal.pcbi.1004591`.

[9] Barabási AL, Gulbahce N, Loscalzo J. Network medicine: a network-based approach to human disease. *Nat Rev Genet*, 2011. **12**(1):56–68. doi:10.1038/nrg2918.

[10] Renatino Canevarolo R, Sudalagunta PR, Coelho Siqueira Silva MD, Meads MB, Granados P, Berglund A, Kulkarni A, Dai H, Dalton WS, Petre I, Shain KH, Siqueira Silva A. A Systems Biology Approach to Identify Mechanisms of Therapy Resistance in Multiple Myeloma. *Blood*, 2018. **132**(Supplement 1):3266–3266. doi:10.1182/blood-2018-99-118784. URL `https://doi.org/10.1182/blood-2018-99-118784`.

[11] Meads MB, Renatino Canevarolo R, Sudalagunta PR, Oliveira PS, Magaletti DM, Fang B, Coelho Siqueira Silva MD, Kulkarni A, Dai H, Dalton WS, Petre I, Koomen JM, Siqueira Silva A, Shain KH. Systems Biology Analysis Identifies Targetable Vulnerability Networks to Proteasome Inhibitors in Multiple Myeloma. *Blood*, 2018. **132**(Supplement 1):950–950. doi:10.1182/blood-2018-99-120269. URL `https://doi.org/10.1182/blood-2018-99-120269`.

[12] Younesi E, Hofmann-Apitius M. From integrative disease modeling to predictive, preventive, personalized and participatory (P4) medicine. *EPMA J*, 2013. **4**(1):23. doi:10.1186/1878-5085-4-23.

[13] Kanhaiya K, Czeizler E, Gratie C, Petre I. Controlling Directed Protein Interaction Networks in Cancer. *Scientific Reports*, 2017. **7**(1):10327. doi:10.1038/s41598-017-10491-y. URL `https://doi.org/10.1038/s41598-017-10491-y`.

[14] Czeizler E, Wu KC, Gratie C, Kanhaiya K, Petre I. Structural Target Controllability of Linear Networks. *IEEE/ACM Transactions on Computational Biology and Bioinformatics*, 2018. **15**(4):1217–1228. doi:10.1109/TCBB.2018.2797271.

[15] Liu YY, Slotine JJ, Barabási AL. Controllability of complex networks. *Nature*, 2011. **473**(7346):167–173. doi:10.1038/nature10011.

[16] Gao J, Liu YY, D'Souza RM, Barabási AL. Target control of complex networks. *Nature Communications*, 2014. **5**:5415. doi:10.1038/ncomms6415.

[17] Guo WF, Zhang SW, Wei ZG, Zeng T, et al. Constrained target controllability of complex networks. *Journal of Statistical Mechanics: Theory and Experiment*, 2017.

[18] Liu YY, Slotine JJ, Barabási AL. Controllability of complex networks. *Nature*, 2011. **473**(7346):167–173. doi:10.1038/nature10011.

[19] Yan G, Vértes PE, Towlson EK, Chew YL, Walker DS, Schafer WR, Barabási AL. Network control principles predict neuron function in the Caenorhabditis elegans connectome. *Nature*, 2017. **550**(7677):519–523. doi:10.1038/nature24056. URL `https://doi.org/10.1038/nature24056`.

[20] Barabási DL, Barabási AL. A Genetic Model of the Connectome. *Neuron*, 2019. doi:https://doi.org/10.1016/j.neuron.2019.10.031. URL `http://www.sciencedirect.com/science/article/pii/S0896627319309262`.

[21] Lohr JG, Stojanov P, Carter SL, Cruz-Gordillo P, Lawrence MS, Auclair D, Sougnez C, Knoechel B, Gould J, Saksena G, Cibulskis K, McKenna A, Chapman MA, Straussman R, Levy J, Perkins LM, Keats JJ, Schumacher SE, Rosenberg M, Getz G, Golub TR. Widespread genetic heterogeneity in multiple myeloma: implications for targeted therapy. *Cancer Cell*, 2014. **25**(1):91–101. doi:10.1016/j.ccr.2013.12.015.

[22] Kalman RE, Ho YC, Narendra KS. Controllability of linear dynamical systems. *Contributions to Differential Equations*, 1963. **1**:189–213.

[23] Gunning R, Rossi H. Analytic functions of several complex variables. Prentice-Hall, 1965.

[24] Lin CT. Structural controllability. *IEEE Trans. Automat. Contr*, 1974. **19**:201–208.

[25] Poljak S, Murota K. Note on a graph-theoretic criterion for structural output controllability. *IEEE Transactions on Automatic Control*, 1990. **35**(8):939—942. doi:10.1109/9.58507.

[26] Wishart DS, Feunang YD, Guo AC, Marcu A, et al. DrugBank 5.0: a major update to the DrugBank database for 2018. *Nucleic Acids Research*, 2017. **46**:1074–1082. doi:10.1093/nar/gkx1037.

[27] Kanhaiya K, Rogojin V, Kazemi K, Czeizler E, Petre I. NetControl4BioMed: a pipeline for biomedical data acquisition and analysis of network controllability. *BMC Bioinformatics*, 2018. **19**. doi:https://doi.org/10.1186/s12859-018-2177-3.

[28] Wang T, Birsoy K, Hughes NW, Krupczak KM, Post Y, Wei JJ, Lander ES, Sabatini DM. Identification and characterization of essential genes in the human genome. *Science*, 2015. **350**(6264):1096–1101. doi:10.1126/science.aac7041.

[29] Blomen VA, Majek P, Jae LT, Bigenzahn JW, Nieuwenhuis J, Staring J, Sacco R, van Diemen FR, Olk N, Stukalov A, Marceau C, Janssen H, Carette JE, Bennett KL, Colinge J, Superti-Furga G, Brummelkamp TR. Gene essentiality and synthetic lethality in haploid human cells. *Science*, 2015. **350**(6264):1092–1096. doi:10.1126/science.aac7557.

[30] Hart T, Chandrashekhar M, Aregger M, Steinhart Z, Brown KR, MacLeod G, Mis M, Zimmermann M, Fradet-Turcotte A, Sun S, Mero P, Dirks P, Sidhu S, Roth FP, Rissland OS, Durocher D, Angers S, Moffat J. High-Resolution CRISPR Screens Reveal Fitness Genes and Genotype-Specific Cancer Liabilities. *Cell*, 2015. **163**(6):1515–1526. doi:10.1016/j.cell.2015.11.015.

[31] Koh JLY, Brown KR, Sayad A, Kasimer D, Ketela T, Moffat J. COLT-Cancer: functional genetic screening resource for essential genes in human cancer cell lines. *Nucleic Acids Res*, 2012. **40**(Database issue):D957–63. doi:10.1093/nar/gkr959.

[32] Matthews GM, de Matos Simoes R, Hu Y, Sheffer M, et al. Characterization of lineage vs. context-dependent essential genes in multiple myeloma using CRISPR-Cas9 genome editing. *Cancer Research*, 2017. **77**(13). doi:10.1158/1538-7445.AM2017-LB-118.

[33] Tiedemann RE, Zhu YX, Schmidt J, Shi CX, et al. Identification of Molecular Vulnerabilities in Human Multiple Myeloma Cells by RNA Interference Lethality Screening of the Druggable Genome. *Cancer Research*, 2012. **72**. doi:10.1158/0008-5472.CAN-11-2781.

[34] Krönke J, Hurst SN, Ebert BL. Lenalidomide induces degradation of IKZF1 and IKZF3. *Oncoimmunology*, 2014. **3**(7). doi:10.4161/21624011.2014.941742.

[35] S K, J C, T C, A G, et al. PubChem 2019 update: improved access to chemical data. *Nucleic Acids Research*, 2018. **47**:1102–1109. doi:10.1093/nar/gky1033.

[36] Kanehisa M, Goto S. KEGG: kyoto encyclopedia of genes and genomes. *Nucleic Acids Res*, 2000. **28**(1):27–30. doi:10.1093/nar/28.1.27.

[37] Türei D, Korcsmáros T, Saez-Rodriguez J. OmniPath: guidelines and gateway for literature-curated signaling pathway resources. *Nature Methods*, 2016. **13**(12):966–967. doi:10.1038/nmeth.4077. URL `https://doi.org/10.1038/nmeth.4077`.

[38] Breuer K, Foroushani AK, Laird MR, Chen C, Sribnaia A, Lo R, Winsor GL, Hancock REW, Brinkman FSL, Lynn DJ. InnateDB: systems biology of innate immunity and beyond–recent updates and continuing curation. *Nucleic Acids Res*, 2013. **41**(Database issue):D1228–33. doi:10.1093/nar/gks1147.

[39] Licata L, Lo Surdo P, Iannuccelli M, Palma A, Micarelli E, Perfetto L, Peluso D, Calderone A, Castagnoli L, Cesareni G. SIGNOR 2.0, the SIGnaling Network Open Resource 2.0: 2019 update. *Nucleic Acids Research*, 2019. doi:10.1093/nar/gkz949. Gkz949, `http://oup.prod.sis.lan/nar/advance-article-pdf/doi/10.1093/nar/gkz949/30324784/gkz949.pdf`, URL `https://doi.org/10.1093/nar/gkz949`.

[40] 2019. URL `https://oldnetcontrol.combio.org/`.

[41] URL `https://tinyurl.com/sjofthz`.

[42] Shannon P, Markiel A, Ozier O, Baliga NS, et al. Cytoscape: a software environment for integrated models of biomolecular interaction networks. *Genome Research*, 2003. pp. 2498–2504. doi:10.1101/gr.1239303.

[43] Liu Y, Zhang Y, Wu H, Li Y, Zhang Y, Liu M, Li X, Tang H. miR-10a suppresses colorectal cancer metastasis by modulating the epithelial-to-mesenchymal transition and anoikis. *Cell Death Dis*, 2017. **8**(4):e2739. doi:10.1038/cddis.2017.61.

[44] Hashimoto Y, Shiina M, Tanaka Y, Dasgupta P, Kulkarni P, Kato T, Wong RK, Shahryari V, Maekawa S, Yamamura S, Bhagiratha D, Saini S, Deng G, Tabatabai L, Majid S, Dahiya R, Dahiya R. Abstract 761: Up-regulation of miR-10a affect on prostate cancer racial disparity. *Cancer Research*, 2019. **79**(13 Supplement):761–761. doi:10.1158/1538-7445.AM2019-761. https://cancerres.aacrjournals.org/content, URL https://cancerres.aacrjournals.org/content/79/13_Supplement/761.

[45] Umezu T, Imanishi S, Yoshizawa S, Kawana C, Ohyashiki JH, Ohyashiki K. Induction of multiple myeloma bone marrow stromal cell apoptosis by inhibiting extracellular vesicle miR-10a secretion. *Blood Adv*, 2019. **3**(21):3228–3240. doi:10.1182/bloodadvances.2019000403.

[46] Umezu T, Imanishi S, Yoshizawa S, Kawana C, Ohyashiki JH, Ohyashiki K. Induction of multiple myeloma bone marrow stromal cell apoptosis by inhibiting extracellular vesicle miR-10a secretion. *Blood Advances*, 2019. **3**(21):3228–3240. doi:10.1182/bloodadvances.2019000403. https://ashpublications.org/bloodadvances/article-pdf/3/21/3228/1506257/advancesadv2019000403.pdf, URL https://doi.org/10.1182/bloodadvances.2019000403.

[47] Neumann C, Zehentmaier G, Danhauser-Riedl S, Emmerich B, Hallek M. Interleukin-6 induces tyrosine phosphorylation of the Ras activating protein Shc, and its complex formation with Grb2 in the human multiple myeloma cell line LP-1. *Eur J Immunol*, 1996. **26**(2):379–384. doi:10.1002/eji.1830260217.

[48] Wang M, Wu D, Liu P, Deng J. Silence of MCL-1 upstream signaling by shRNA abrogates multiple myeloma growth. *Experimental Hematology & Oncology*, 2014. **3**(1):27. doi:10.1186/2162-3619-3-27. URL https://doi.org/10.1186/2162-3619-3-27.

[49] S P, C T, P T, G G, D D, V M, C B, C S, A C, H E. KRAS/NRAS/BRAF Mutations as Potential Targets in Multiple Myeloma. *Front. Oncol.*, 2019. **9**(1137).

[50] Chen X, Liu Y, Yang Z, Zhang J, Chen S, Cheng J. LINC01234 promotes multiple myeloma progression by regulating miR-124-3p/GRB2 axis. *American journal of translational research*, 2019. **11**(10):6600–6618. URL https://www.ncbi.nlm.nih.gov/pubmed/31737211.

[51] Johnston JR, Chase PB, Pinto JR. Troponin through the looking-glass: emerging roles beyond regulation of striated muscle contraction. *Oncotarget*, 2017. **9**(1):1461–1482. doi:10.18632/oncotarget.22879. URL https://www.ncbi.nlm.nih.gov/pubmed/29416706.

[52] Sun Z, Schwenzer A, Rupp T, Murdamoothoo D, Vegliante R, Lefebvre O, Klein A, Hussenet T, Orend G. Tenascin-C Promotes Tumor Cell Migration and Metastasis through Integrin ?91-Mediated YAP Inhibition. *Cancer research*, 2018. **78**(4):950–961. doi:10.1158/0008-5472.CAN-17-1597. URL https://www.ncbi.nlm.nih.gov/pubmed/29259017.

[53] Chen Y, Huang R, Ding J, Ji D, Song B, Yuan L, Chang H, Chen G. Multiple myeloma acquires resistance to EGFR inhibitor via induction of pentose phosphate pathway. *Scientific Reports*, 2015. **5**(1):9925. doi:10.1038/srep09925. URL https://doi.org/10.1038/srep09925.

[54] Barabasi, Albert. Emergence of scaling in random networks. *Science*, 1999. **286**(5439):509–512. doi:10.1126/science.286.5439.509.

[55] Júlvez J, Vázquez CR, Mahulea C, Silva M. Continuous Petri Nets: Controllability and Control, pp. 407–428. Springer London, London. ISBN 978-1-4471-4276-8, 2013. doi:10.1007/978-1-4471-4276-8{_}20. URL https://doi.org/10.1007/978-1-4471-4276-8_20.

[56] Carvalho RV, Kleijn J, Meijer AH, Verbeek FJ. Modeling innate immune response to early Mycobacterium infection. *Comput Math Methods Med*, 2012. **2012**:790482. doi:10.1155/2012/790482.